Optimum Noncoherent Multiuser Detection for DPSK Modulation in Generalized Diversity Rayleigh Fading Channels: An Asymptotic Minimum Error Probability Analysis

Matthias Brehler and Mahesh K. Varanasi
e-mail: {brehler, varanasi}@dsp.colorado.edu
University of Colorado, Boulder, CO 80309

Abstract — **The jointly optimum noncoherent multiuser detector for DPSK modulation in generalized diversity Rayleigh fading channels (GDRF) was presented in [1] and bounds on the error probability were obtained. In the numerical examples of [1] these bounds were seen to converge. This paper examines analytically the behavior of the bounds for high signal-to-noise ratio (SNR) scenarios. Slowly fading channels, where the fading coefficients are essentially constant over two successive symbol intervals, and fast fading channels, where the fading coefficients can vary from one symbol interval to the next, are considered.**

For slow fading, the asymptotic convergence of the upper bound to the lower bound is proved. The asymptote that is reached for high values of the SNR does not depend on the interfering users' energies, establishing thereby the near-far resistance of the optimum multiuser DPSK detector. For fast fading the error floor reached for high SNRs is bounded from below and above.

I. Introduction

A systematic approach to detection for DPSK modulated signals in generalized diversity Rayleigh fading (GDRF) channels was introduced in [2], where the single-user detection problem was considered (see also [3]). A minimum error probability (MEP) detector and a near-optimum generalized likelihood ratio test (GLRT) detector were derived and analyzed. The GDRF channel model introduced in [2], [3] covers not only frequency-selective fading (arising from multiple signal paths), but also other forms of diversity: it subsumes and generalizes previous diversity models and is also applicable to antenna or other diversity methods (cf. [3]). The single-user results in [2] and [3] were also applied to post-combining decorrelative multiuser detection. However, decorrelating-type detectors are sub-optimal.

The optimum multiuser MEP and GLRT detectors were obtained in [1], extending the approach of [2] to the multiuser case. Since an exact error probability analysis is intractable, upper and lower bounds on the error probability of the MEP and the GLRT detectors were derived [1]. In this paper we undertake an asymptotic (high SNR) error probability analysis for the multiuser MEP detector. This analysis was first presented in a technical report and a thesis [4].

The asymptotic analysis considers both slow and fast fading. In the context of DPSK modulation we define slow fading to mean that the fading coefficients are constant over at least two consecutive symbol intervals. In fast fading the fading coefficients are assumed to be essentially constant over one symbol interval but can change from one symbol interval to the next. For slow fading the asymptotic analysis reveals that our upper and lower bounds on the error probability always converge for high signal-to-noise ratios (SNR). As the lower bound results from only considering the single error event (an error occurs only for the user of interest), the asymptote is independent of the interfering users' energies.

The following three sections revisit briefly material presented in more detail in [1]: the discrete multiuser GDRF channel model is presented in Section II, and the derivation of the MEP detector is outlined in Section III. Section IV-A repeats briefly the derivation of the upper and lower bound on bit error probability. The asymptotic behavior of the bounds for high SNR scenarios is examined in Section IV-B. Numerical examples are given in Section V, and conclusions are drawn in Section VI.

II. Discrete-Time Model for the Multiuser Generalized Diversity Rayleigh Fading Channel

Corresponding to [1], we present the discrete-time model for the K user, L diversity branches GDRF channel. It is a direct extension of the single user model in [2] and [3]. The KL-dimensional vectors of observations for the zeroth and the previous symbol interval can be written as

$$\mathbf{q}(-1) = \sqrt{\bar{\gamma}}\boldsymbol{\mathcal{R}}\boldsymbol{\Omega}^{1/2}\mathbf{D}(-1)\mathbf{c}(-1)+\mathbf{n}(-1), \quad (1)$$

$$\mathbf{q}(0) = \sqrt{\bar{\gamma}}\boldsymbol{\mathcal{R}}\boldsymbol{\Omega}^{1/2}\mathbf{D}(0)\mathbf{c}(0)+\mathbf{n}(0), \quad (2)$$

where $\bar{\gamma}$ is the average signal to noise ratio (SNR) of user one and $\boldsymbol{\Omega} = \mathrm{diag}\{\mathbf{r}\} \otimes \mathbf{I}_L$ and $\mathbf{D}(n) = \mathrm{diag}\{\mathbf{d}(n)\} \otimes \mathbf{I}_L$ ($\mathbf{I}_L$ denotes a L dimensional identity matrix and $\otimes$ the Kronecker product). The K-dimensional vector $\mathbf{r}$ contains the K users' average energy ratios relative to user one and the vectors $\mathbf{d}(0)$ and $\mathbf{d}(-1)$ contain the differentially encoded symbols of the K users at the zeroth and previous symbol interval. Each element of $\mathbf{d}(-1)$, $\mathbf{d}(0)$ belongs to an MPSK constellation $F = \{\mathrm{e}^{\frac{j2\pi l}{M}}\}_{l=0}^{M-1}$ and the k^{th} element of the K-dimensional vector of information symbols $\mathbf{b}(0) \in F^K$ is related to the differentially encoded symbols by $d_k(0) = d_k(-1)\, b_k(0)$.

The matrix $\boldsymbol{\mathcal{R}}$ is the $KL \times KL$ dimensional generalized signal correlation matrix of the K users' signature signals and the (possibly correlated) L diversity waveforms of each such signal (for example the time translates of the signature signals in L resolvable paths of a multipath channel). Each user's signal is normalized so that the diagonal elements of $\boldsymbol{\mathcal{R}}$ are unity. Possible inter-symbol-interference (ISI) is eliminated by masking out the signal for the relevant times as described in [5].

The KL-dimensional vector of fading channel coefficients $\mathbf{c}(n)$ is defined via $\mathbf{c}^{\mathsf{T}}(n) = [\mathbf{c}_1^{\mathsf{T}}(n),\ \ldots,\ \mathbf{c}_K^{\mathsf{T}}(n)]$, where $\mathbf{c}_k(n)$ contains the L fading coefficients of the k^{th} user's L diversity branches during the n^{th} symbol interval. Both, $\mathbf{c}(n)$ and the additive noise vectors $\mathbf{n}(n)$, are zero-mean, complex, circularly symmetric Gaussian random vectors. Whereas $\mathbf{n}(-1)$ and $\mathbf{n}(0)$ are statistically independent and have an identical correlation matrix $E[\mathbf{n}(n)\mathbf{n}^{\dagger}(n)] = \boldsymbol{\mathcal{R}}$ the vectors of the fading parameters $\mathbf{c}(-1)$ and $\mathbf{c}(0)$ are not statistically independent († denotes the conjugate complex transpose). Their

This work was supported in part by NSF Grant ANI-9725778.

matrix correlation function $E[\mathbf{c}(n)\mathbf{c}^\dagger(m)]$ is denoted as $\mathbf{\Sigma}(n,m)$; the k^{th} $L \times L$ submatrix of $\mathbf{\Sigma}(n,m)$, $\mathbf{\Sigma}_{kk}(n,m)$, is the correlation matrix of the k^{th} user's fading parameters. To keep the analysis in this paper tractable we assume that the fading paths of different users are statistically independent of each other, i.e., $\mathbf{\Sigma}(n,m)$ is block-diagonal with $\mathbf{\Sigma}_{kk}(n,m)$ as diagonal elements. Wide sense stationarity of the fading process allows us to write $\mathbf{\Sigma}(n,n) = \mathbf{\Sigma}(0)$ and $\mathbf{\Sigma}(-1,0) = \mathbf{\Sigma}^\dagger(0,-1) = \mathbf{\Sigma}(1)$. For the slowly fading channel (fading coefficients do not change for the duration of two successive symbol intervals) $\mathbf{\Sigma}(-1,0) = \mathbf{\Sigma}(0,-1) = \mathbf{\Sigma}(0)$. In order to ensure that $\bar{\gamma}r_k$ is the total average received signal to noise ratio of user k, the matrices $\mathbf{\Sigma}_{kk}$ are normalized such that $\mathrm{tr}(\mathbf{\Sigma}_{kk}\mathbf{R}_{kk}) = 1$, where $\mathbf{R}_{kk}$ is the k^{th} $L \times L$ sub-matrix of $\boldsymbol{\mathcal{R}}$ (the k^{th} user's signal correlation matrix).

III. The Minimum Probability of Error (MEP) Detector

The decision rule for the minimum error probability (MEP) detector for the joint detection of all K users was derived in [1]. It was shown there that under the assumption of independent fading processes of the different users the likelihood of the observations depends only on the M^K possible combinations of data-symbols $\mathbf{b}(0)$ and not on all M^{2K} combinations of differentially encoded symbols $(\mathbf{d}(-1), \mathbf{d}(0))$. In what follows, it is convenient to drop the time index in $\mathbf{b}(0)$ and introduce the integer subscript i ($1 \le i \le M^K$) indicating the dependence of the transmitted data symbols on the underlying hypothesis H_i. Hence, H_i designates the hypothesis that $\mathbf{b}_i$ is the particular realization of the vector of data symbols $\mathbf{b}(0)$. Furthermore, we define $\mathbf{B}_i = \mathrm{diag}\{\mathbf{b}_i\} \otimes \mathbf{I}_L$ and stack the vectors of observations to define $\mathbf{q}^\mathsf{T} = \begin{bmatrix} \mathbf{q}^\mathsf{T}(-1) & \mathbf{q}^\mathsf{T}(0) \end{bmatrix}$. In [1] we derived the MEP decision rule in the statistics $\mathbf{q}$. For the purpose of this paper it is more convenient to state the decision rule in the decorrelated statistics $\mathbf{z}$, where $\mathbf{z}$ is defined as $\mathbf{z} = \left(\mathbf{I}_2 \otimes \boldsymbol{\mathcal{R}}^{-1}\right)\mathbf{q}$. The covariance matrix of the new decision statistics $\mathbf{z}$ becomes

$$\mathbf{K}_{\mathbf{z}|H_i} = E[\mathbf{z}\mathbf{z}^\dagger] = \begin{bmatrix} \bar{\gamma}\mathbf{\Omega}\mathbf{\Sigma}(-1,-1) + \boldsymbol{\mathcal{Q}} & \bar{\gamma}\mathbf{\Omega}\mathbf{\Sigma}(-1,0)\mathbf{B}_i^* \\ \bar{\gamma}\mathbf{B}_i\mathbf{\Sigma}(0,-1)\mathbf{\Omega} & \bar{\gamma}\mathbf{\Omega}\mathbf{\Sigma}(0,0) + \boldsymbol{\mathcal{Q}} \end{bmatrix}, \tag{3}$$

where $\boldsymbol{\mathcal{Q}} = \boldsymbol{\mathcal{R}}^{-1}$. Note that in the above matrices the product of $\mathbf{\Sigma}(n,m)$ and $\mathbf{\Omega}$ commutes, because $\mathbf{\Sigma}(n,m)$ is block-diagonal with blocks of size $L \times L$ and each element of $\mathbf{r}$ is repeated L times on the diagonal of $\mathbf{\Omega}$. The MEP decision rule can then be stated in the statistics $\mathbf{z}$ as

$$\hat{i} = \arg \min_{i \in \{1,\,2,\,\ldots,\,M^K\}} \mathbf{z}^\dagger\, \mathbf{K}_{\mathbf{z}|H_i}^{-1}\, \mathbf{z} + \ln\left(\left|\mathbf{K}_{\mathbf{z}|H_i}\right|\right), \tag{4}$$

where for any matrix $\mathbf{M}$ we define $|\mathbf{M}| = \det(\mathbf{M})$.

IV. Error Probability Analysis

To keep the analysis simple, we restrict ourselves to binary modulation. Even with this restriction, an exact computation of the error probability is intractable. Therefore we give a lower and upper bound on the error probability of the MEP detector in [1]. After a brief review of these bounds, we proceed by showing the asymptotic convergence of the bounds for the slowly fading case in Section IV-B.1 and give bounds on the error floor for fast fading in Section IV-B.2. Without loss of generality, the error probability of the first user is considered.

A. Bounds on Error Probability

An upper bound on the error probability of user one is derived by invoking a union bound and a lower bound by exclusively considering the single error event when only an error for user one occurs. To derive these bounds we first consider the probability that a hypothesis H_i is detected as H_j, which we denote as $P_{H_i \to H_j}$. Hence, $P_{H_i \to H_j}$ is the probability that (4) is minimized by $\mathbf{b}_j$ rather than by the transmitted data symbols $\mathbf{b}_i$. This probability can be expressed as the probability that a single quadratic form in the decision statistics is smaller than some constant (cf. [1], [6])

$$P_{H_i \to H_j} = \Pr\left(\mathbf{z}^\dagger \mathbf{F}_{ij}\mathbf{z} < c_{ij}\,|H_i\right), \tag{5}$$

where $\mathbf{F}_{ij} = \left(\mathbf{K}_{\mathbf{z}|H_j}^{-1} - \mathbf{K}_{\mathbf{z}|H_i}^{-1}\right)$ and $c_{ij} = \ln\left(\left|\mathbf{K}_{\mathbf{z}|H_i}\right| / \left|\mathbf{K}_{\mathbf{z}|H_j}\right|\right)$. In the remainder of this section, we state all expressions in terms of $\mathbf{F}_{ij}$, c_{ij}, and the covariance matrix $\mathbf{K}_{\mathbf{z}|H_i}$ of the decision statistics $\mathbf{z}$. As $\mathbf{F}_{ij}$ is Hermitian and $\mathbf{z}$ is a zero-mean, complex Gaussian random vector the characteristic function of the quadratic form $\mathbf{z}^\dagger\mathbf{F}_{ij}\mathbf{z}$ is given in Appendix B of [7] as

$$E\left[e^{-s\mathbf{z}^\dagger\mathbf{F}_{ij}\mathbf{z}}\right] = \frac{1}{\prod_{l=1}^{l=N} \lambda_l^{\mu_l}\left(s + \frac{1}{\lambda_l}\right)^{\mu_l}}, \tag{6}$$

where N is the number of distinct, non-zero eigenvalues $\{\lambda_l\}_{l=1}^N$ with multiplicities $\{\mu_l\}_{l=1}^N$ of $\mathbf{K}_{\mathbf{z}|H_i}\mathbf{F}_{ij}$.

Without loss of generality we assume that the M eigenvalues $\lambda_1, \lambda_2, \ldots, \lambda_M$ are negative and that the $N-M$ eigenvalues $\lambda_{M+1}, \lambda_{M+2}, \ldots, \lambda_N$ are positive. With the help of this, the probability $P_{H_i \to H_j}$ may be expressed in the form (see also [6])

$$P_{H_i \to H_j} = -\sum_{m=1}^{M} \mathrm{Res}\left(\frac{\mathrm{e}^{sc_{ij}}}{s\prod_{l=1}^{l=N}\lambda_l^{\mu_l}\left(s+\frac{1}{\lambda_l}\right)^{\mu_l}},\; s_m = \frac{-1}{\lambda_m}\right) \tag{7}$$

for $c_{ij} \le 0$. For $c_{ij} > 0$ the probability is calculated as

$$P_{H_i \to H_j} = 1 + \sum_{m=M+1}^{N} \mathrm{Res}\left(\frac{\mathrm{e}^{sc_{ij}}}{s\prod_{l=1}^{l=N}\lambda_l^{\mu_l}\left(s+\frac{1}{\lambda_l}\right)^{\mu_l}},\; s_m = \frac{-1}{\lambda_m}\right). \tag{8}$$

In both equations the residue of a function $f(s)$ in a pole a of multiplicity m is defined to be

$$\mathrm{Res}\,(f(s),\,a) = \frac{1}{(m-1)!}\,\lim_{s \to a}\frac{d^{m-1}}{ds^{m-1}}\left[(s-a)^m f(s)\right]. \tag{9}$$

This notation is especially convenient for poles of multiplicity greater than one, which we will encounter in the following sections.

Having obtained the probability $P_{H_i \to H_j}$, we invoke a union bound on the error probability of user one, given a specific hypothesis H_i was transmitted, denoted as $P_{e|H_i}$. Computing $P_{e|H_i}$ precisely would require the evaluation of the probability of the union of all 2^{K-1} possible error events where an error for user one occurs. The probability of the union of events is upper bounded by the sum of the probabilities of these error events. Averaging over all 2^K equally probable hypotheses H_i yields the upper bound on the first user's error probability P_e

$$P_e \le \frac{1}{2^K}\sum_{i=1}^{2^K} \sum_{\substack{\forall j \in \{1,\,\ldots,\,2^K\}\ \mathrm{s.t.} \\ [\mathbf{b}_j]_1 \ne [\mathbf{b}_i]_1}} P_{H_i \to H_j}, \tag{10}$$

where $[\mathbf{b}_i]_k$ denotes the k^{th} element of the vector of data symbols corresponding to hypothesis H_i. $[\mathbf{b}_i]_1 \neq [\mathbf{b}_j]_1$ indicates the error in the detection of the first user's data symbol because only error events with possible multiple errors are considered where an error for the first user occurs.

A lower bound on the first user's error probability is simply obtained by averaging over all 2^K single error events for the first user

$$P_e \geq \frac{1}{2^K} \sum_{\substack{i=1 \\ j \text{ s.t. } [\mathbf{b}_j]_1 \neq [\mathbf{b}_i]_1 \\ [\mathbf{b}_i]_k = [\mathbf{b}_j]_k,\ 2 \leq k \leq K}}^{2^K} P_{H_i \to H_j}. \tag{11}$$

By this, and equations (7), (8), and (10) the bounds on the first user's error probability are fully specified, and we can proceed to show the behavior of these bounds for high SNR.

B. Asymptotic Error Probability Analysis

Applying the results of [6], we only need to find the asymptotic (high SNR) eigenvalues of $\mathbf{C}_{ij} = \mathbf{K}_{\mathbf{z}|H_i}\mathbf{F}_{ij} = \mathbf{K}_{\mathbf{z}|H_i}\mathbf{K}_{\mathbf{z}|H_j}^{-1} - \mathbf{I}$ to find the asymptotic expression for $P_{H_i \to H_j}$. To this end, we will first state some definitions and then reveal the results of the asymptotic analysis for the MEP in separate subsections for slow and fast fading. We will find that the bounds on the error probability converge asymptotically for high SNR in the case of slow fading whereas for fast fading we will only be able to bound the error floor from below and above; numerical examples show that these bounds are still tight.

The asymptotic analysis of the MEP detector is only presented for a special case of the fading parameters' covariance matrix, i.e., $\mathbf{\Sigma}(-1,0) = \mathbf{\Sigma}(0,-1) = \rho\mathbf{\Sigma}(0)$. The correlation coefficient ρ characterizes the fade rate of the channel and is connected to the normalized Doppler bandwidth $B_D T$ for example by $\rho = J_0(\pi B_D T)$ (J_0 is the Bessel function of the first kind of order 0) for fading with power spectrum density according to Jakes's model [8]. ρ equal to one corresponds to the slowly fading channel for which the fading coefficients stay constant over two successive symbol intervals. ρ smaller than one specifies the fast fading channel in the context of this analysis. The above restriction on the fading parameters' covariance matrices implies that all users suffer from the same fade rate. This is applicable for slow fading (systems specified by high data rates and/or slow velocities) but is unrealistic for fast fading, because it implies that the relative movement between the transmitter and all users is the same. However, the basic behavior of the detector is very well captured with this simplifying assumption and the analysis is easily extended to different fade rates for each user.

For the remaining analysis we will just consider hypotheses H_i, H_j whose corresponding vectors of data symbols have the following structure

$$\begin{aligned} \mathbf{b}_i^\mathsf{T} &= \left[\ -\mathbf{1}_{e_{ij-}}^\mathsf{T}\ +\mathbf{1}_{e_{ij+}}^\mathsf{T}\ +\mathbf{1}_{o_{ij+}}^\mathsf{T}\ -\mathbf{1}_{o_{ij-}}^\mathsf{T}\ \right], \\ \mathbf{b}_j^\mathsf{T} &= \left[\ +\mathbf{1}_{e_{ij-}}^\mathsf{T}\ -\mathbf{1}_{e_{ij+}}^\mathsf{T}\ +\mathbf{1}_{o_{ij+}}^\mathsf{T}\ -\mathbf{1}_{o_{ij-}}^\mathsf{T}\ \right], \end{aligned} \tag{12}$$

where $\mathbf{1}_n$ is an n length vector containing n ones and $e_{ij+} + e_{ij-} + o_{ij+} + o_{ij-} = K$ and $e_{ij+} + e_{ij-} = e_{ij}$, the number of occurred errors. This ordering procedure can be performed without loss of generality because for any error event $(\tilde{H}_i \to \tilde{H}_j)$ with arbitrary ordering we can reorder the users according to the above scheme, rearrange the users' signal correlation matrix $\boldsymbol{\mathcal{R}}$, and the correlation matrix of the decision statistics $\mathbf{K}_{\mathbf{z}|H_i}$ and hence calculate the error probability of the corresponding error event $(H_i \to H_j)$. The reordering corresponds to inserting permutation matrices in (1) and (2).

To be more precise about the above notation, we define an error vector $\mathbf{e}_{ij}$ as $\mathbf{e}_{ij} = \frac{1}{2}(\mathbf{b}_i - \mathbf{b}_j)$ and the error weight e_{ij} as the sum of the absolute values of the elements of $\mathbf{e}_{ij}$. As indicated in (12) we assume that all errors of an error event $(H_i \to H_j)$ occur within the first e_{ij} users and furthermore, that the first e_{ij-} elements of $\mathbf{e}_{ij}$ are minus unity and the following e_{ij+} elements are plus unity where of course $e_{ij} = e_{ij-} + e_{ij+}$. Additionally, we also order the $K - e_{ij}$ remaining users for which no error occurs in a way that the first o_{ij+} users send $+1$ and the next o_{ij-} users send -1.

With the help of the above ordering we define a 4×4 matrix partitioning of any $KL \times KL$ matrix $\mathbf{M}$ where the diagonal elements have the following dimensions: $\text{size}(\mathbf{M}_{11}) = e_{ij-}L \times e_{ij-}L$, $\text{size}(\mathbf{M}_{22}) = e_{ij+}L \times e_{ij+}L$, $\text{size}(\mathbf{M}_{33}) = o_{ij+}L \times o_{ij+}L$, and $\text{size}(\mathbf{M}_{44}) = o_{ij-}L \times o_{ij-}L$. All other entries have appropriate dimensions. Every matrix subscript in the following sections on the asymptotic analysis refers to the submatrix according to this partitioning, unless stated otherwise. Furthermore, a subscript on $[\cdot]$ refers to the corresponding submatrix of the expression in brackets according to this partitioning.

B.1 Asymptotic Analysis for Slow Fading

For the slowly fading case ($\rho = 1$), we will find, that the eigenvalues of $\mathbf{C}_{ij}$ will be zero with multiplicity $2(K - e_{ij})L$, minus unity with multiplicity $e_{ij}L$, and $e_{ij}L$ times positive and linear in $\bar{\gamma}$ for large $\bar{\gamma}$. This will establish the dominance of the single error event and thus the asymptotic convergence of the upper bound to the lower bound.

Using the matrix inversion lemma (cf. [9]) on $\mathbf{K}_{\mathbf{z}|H_j}$ as it is partitioned in (3) allows us to calculate $\mathbf{C}_{ij} = \mathbf{K}_{\mathbf{z}|H_i}\mathbf{K}_{\mathbf{z}|H_j}^{-1} - \mathbf{I}$. $\mathbf{C}_{ij}$ is a 2×2 block partitioned matrix with two identical blocks $\mathbf{A}$ on the diagonal and two identical blocks $\mathbf{B}$ on the off-diagonals. The eigenvalues of a matrix of this form are equal to the eigenvalues of $\mathbf{A} + \mathbf{B}$ and $\mathbf{A} - \mathbf{B}$. Once $\mathbf{A} \pm \mathbf{B}$ is calculated and terms tending to zero for SNR to infinity are neglected, it can be shown that for high SNR $\mathbf{C}_{ij}$ has the above claimed multiplicities of eigenvalues 0 and -1. Furthermore, $e_{ij-}L$ eigenvalues of $\mathbf{C}_{ij}$ are arbitrarily close (for $\bar{\gamma} \to \infty$) to the eigenvalues of the matrix $\bar{\gamma}2\left[\mathbf{\Omega}\mathbf{\Sigma}(0)\left(\boldsymbol{\mathcal{Q}} + \mathbf{B}_j\boldsymbol{\mathcal{Q}}\mathbf{B}_j\right)^{-1}\right]_{11}$ and $e_{ij+}L$ eigenvalues approach the eigenvalues of the matrix $\bar{\gamma}2\left[\mathbf{\Omega}\mathbf{\Sigma}(0)\left(\boldsymbol{\mathcal{Q}} + \mathbf{B}_j\boldsymbol{\mathcal{Q}}\mathbf{B}_j\right)^{-1}\right]_{22}$. It is left to show that the eigenvalues of these matrices are always positive. It is not hard to prove that

$$\left[\left(\boldsymbol{\mathcal{Q}} + \mathbf{B}_j\boldsymbol{\mathcal{Q}}\mathbf{B}_j\right)^{-1}\right]_{11} = \frac{1}{2}\left(\boldsymbol{\mathcal{Q}}_{11} - \boldsymbol{\mathcal{Q}}_{13}\boldsymbol{\mathcal{Q}}_{33}^{-1}\boldsymbol{\mathcal{Q}}_{31}\right)^{-1}, \tag{13}$$

where the right-hand side is positive definite because it is a Schur complement of the positive definite matrix $\boldsymbol{\mathcal{Q}}$ (recall $\boldsymbol{\mathcal{Q}} = \boldsymbol{\mathcal{R}}^{-1}$). A similar expression is available for $\left[\left(\boldsymbol{\mathcal{Q}} + \mathbf{B}_j\boldsymbol{\mathcal{Q}}\mathbf{B}_j\right)^{-1}\right]_{22}$, which is hence also positive definite. Furthermore, as $\mathbf{\Omega}$ and $\mathbf{\Sigma}(0)$ are block-diagonal with block size $L \times L$ and the partitioning proposed above has block sizes that are integer multiples of L, we can write $\left[\mathbf{\Omega}\mathbf{\Sigma}(0)\left(\boldsymbol{\mathcal{Q}} + \mathbf{B}_j\boldsymbol{\mathcal{Q}}\mathbf{B}_j\right)^{-1}\right]_{11} = [\mathbf{\Omega}]_{11}[\mathbf{\Sigma}(0)]_{11}\left[\left(\boldsymbol{\mathcal{Q}} + \mathbf{B}_j\boldsymbol{\mathcal{Q}}\mathbf{B}_j\right)^{-1}\right]_{11}$. As $[\mathbf{\Omega}]_{11}$ contains the energy ratios of the users, it is positive definite and so is the diagonal block of the correlation matrix $\mathbf{\Sigma}(0)$. Thus the $e_{ij}L$ eigenvalues linear in $\bar{\gamma}$ are all positive, establishing the remainder of the above claim.

It can also be shown that the value of c_{ij} approaches a constant $\hat{c}_{ij}$ for large SNR; the constant can be smaller or greater than zero (a closed form expression for $\hat{c}_{ij}$ is available but of minor interest here). Using the aforementioned properties of the eigenvalues and $\hat{c}_{ij}$, we can now apply [6, Proposition 2] and approximate the probability $P_{H_i \to H_j}$ given in (7) for non-positive $\hat{c}_{ij}$ and large $\bar{\gamma}$ as

$$P_{H_i \to H_j} \approx \frac{\mathrm{e}^{\hat{c}_{ij}} \sum_{k=0}^{e_{ij}L-1} \binom{2e_{ij}L-1-k}{e_{ij}L} \frac{(-\hat{c}_{ij})^k}{k!}}{(2\bar{\gamma})^{e_{ij}L} \left| \left[\mathbf{\Omega\Sigma}(0) \left(\boldsymbol{\mathcal{Q}} + \mathbf{B}_j \boldsymbol{\mathcal{Q}} \mathbf{B}_j\right)^{-1} \right]_{[e_{ij}L \times e_{ij}L]} \right|}, \tag{14}$$

where the subscript $[e_{ij}L \times e_{ij}L]$ denotes the upper left block matrix of size $e_{ij}L \times e_{ij}L$ of the term in brackets (the determinant of this matrix multiplied by $(2\bar{\gamma})^{e_{ij}L}$ is equivalent of the product of all positive eigenvalues because the $[\cdot]_{12}$ and $[\cdot]_{21}$ elements of $(\boldsymbol{\mathcal{Q}} + \mathbf{B}_j \boldsymbol{\mathcal{Q}} \mathbf{B}_j)^{-1}$ can be shown to be $\mathbf{0}$).

For positive $\hat{c}_{ij}$ we can approximate $P_{H_i \to H_j}$ as [6, Proposition 2]

$$P_{H_i \to H_j} \approx \frac{\sum_{k=0}^{e_{ij}L} \binom{2e_{ij}L-1-k}{e_{ij}L-1} \frac{\hat{c}_{ij}^k}{k!}}{(2\bar{\gamma})^{e_{ij}L} \left| \left[\mathbf{\Omega\Sigma}(0) \left(\boldsymbol{\mathcal{Q}} + \mathbf{B}_j \boldsymbol{\mathcal{Q}} \mathbf{B}_j\right)^{-1} \right]_{[e_{ij}L \times e_{ij}L]} \right|}. \tag{15}$$

As all probabilities $P_{H_i \to H_j}$ depend on $\bar{\gamma}^{-e_{ij}L}$, and e_{ij} is the number of errors, it can be easily seen that the single error event (only an error for user one occurs, i.e., $e_{ij} = 1$) dominates the error probability, i.e., for high SNR we can neglect all other error events where errors occur also for users other than the first user. Hence, the upper bound converges asymptotically with the lower bound and we can approximate the bit error rate for slow fading (SF) as

$$P_e^{\mathrm{SF}} \approx \frac{1}{2^K} \sum_{\substack{i=1 \\ \forall j \in \{1,\,\ldots,\,2^K\} \text{ s.t. } e_{ij}=1}}^{2^K} P_{H_i \to H_j}\,. \tag{16}$$

From the dominance of the single error event, it is also immediately clear that the MEP detector is near-far resistant, because the probabilities $P_{H_i \to H_j}$ do not depend on the other users energies as $[\mathbf{\Omega}]_{L \times L} = \mathbf{I}$.

B.2 Analysis for Fast Fading

For the fast fading channel it can be shown, using techniques similar to those for the slowly fading channel, that as SNR goes to infinity the eigenvalues of $\mathbf{C}_{ij}$ approach the values $-\frac{2\rho}{1+\rho}$ and $\frac{2\rho}{1-\rho}$ with multiplicity $e_{ij}L$. The constant c_{ij} approaches 0. Inserting these values in the formulae for $P_{H_i \to H_j}$ and performing the necessary derivatives yields (we assume $0 < \rho < 1$)

$$P_{H_i \to H_j} \approx \left(\frac{1-\rho^2}{4}\right)^{e_{ij}L} \sum_{k=1}^{e_{ij}L} \binom{2e_{ij}L-1-k}{e_{ij}L-1} \left(\frac{2}{1+\rho}\right)^k. \tag{17}$$

As the probabilities $P_{H_i \to H_j}$ only depend on the number of errors, and not on the distribution of the errors within the users, the lower bound on the error probability of the MEP detector in fast fading channels is simply (17) with $e_{ij} = 1$. The upper bound becomes

$$\begin{aligned} P_e^{FF} \quad \leq \quad & \sum_{e=1}^{K} \binom{K-1}{e-1} \left(\frac{1-\rho^2}{4}\right)^{eL} \times \\ & \sum_{k=1}^{eL} \binom{2eL-1-k}{eL-1} \left(\frac{2}{1+\rho}\right)^k, \end{aligned} \tag{18}$$

where we dropped the subscript $_{ij}$ as there is no dependence on a specific error event left. Note also that the error floor depends entirely on the fade rate ρ (and the number of users for the upper bound); for high SNR the fading dominates the system behavior, regardless of the signals used.

V. Numerical Results

In this section we present numerical examples. Six users are considered who employ length-31 Gold-sequences as in [1]–[3]. The signal correlation matrix $\boldsymbol{\mathcal{R}}$ is calculated as defined in [5] using the ISI-IUI mask described therein. There are four paths for each user, which fade independently. The average relative power of each fading path is chosen according to the simplified GSM test profile 'urban'. Normalizing $\mathbf{\Sigma}(0)$ properly leads to $\mathbf{\Sigma}(0) = \mathrm{diag}\{0.22,\ 0.42,\ 0.26,\ 0.10\}$. The error probabilities displayed in the figures are not calculated using the residue method used in the analysis above, because this is a numerically unstable method. Instead the inverse Laplace transform is computed numerically using the saddlepoint integration technique. A description of this numerically stable and arbitrarily precise integration method can be found, for example, in [10].

Figure 1 demonstrates the convergence of the upper bound to the lower bound on the bit error rate (BER) of the MEP DPSK multiuser detector. In this example the energies of all users are equal ($r_k = w_k/w_1 = 1\ \forall\, k$). The asymptote the bounds converge to is also displayed. Furthermore, the bit error rates of single-user DPSK MEP and optimum coherent BPSK detection are given as a reference. Note the asymptotic 2dB gap between single and multiuser noncoherent DPSK detection. Since we have derived an asymptotic expression for the BER of the multiuser MEP detector, it is not hard to verify that the asymptotic efficiency of noncoherent DPSK detection is in general smaller than one.

Figure 2 examines the behavior of the bounds for varying interfering users' relative energies at two fixed average SNRs of the first user ($\bar{\gamma}$). For simplicity, all interfering users have the same relative power ($w_k/w_1 =$ const. for $k \geq 2$). Note the independence of the asymptote of the interfering users' energies, illustrating the analytical results. It can also be shown analytically that for vanishing interfering users' energies, the multiuser MEP decision rule simplifies to the single-user decision rule. Hence, it seems reasonable to conjecture that the lower bound captures the true BER of the MEP in regions of small interfering users' energies.

Figure 3 considers fast fading and depicts the bounds on the error floor for $\bar{\gamma} \to \infty$. Even for 100 users the upper bound is tight for relevant values of ρ and more than one fading path. The abscissa in this plot is given in three different scales: the correlation coefficient ρ, $(1-\rho)$(dB), and the normalized Doppler bandwidth $B_D T$ where a power spectrum density according to Jakes's model was chosen. $B_D T$ has to be multiplied with the factor $\frac{c\, r_b}{2\, f_c}$ (c is the speed of light, $r_b = 1/T$ the bit rate, and f_c the carrier frequency) to obtain a corresponding velocity. For a carrier frequency of 9GHz and a bit rate of 20kbs one would have to multiply $B_D T$ with roughly 10^3 to obtain the speed in kilometers per hour.

VI. Conclusions

In this paper we give a rigorous proof for the numerical observation in [1] that the upper and lower bounds on the BER of the MEP detector converge asymptotically for slow fading. The asymptotic tightness of the bounds allows us to quantify the asymptotic BER, near-far resistance, and asymptotic efficiency of noncoherent multiuser DPSK detection in GDRF channels.

Calculating the asymptotic BER for the single-user, slowly fading case (a special case of the multiuser analysis above), reveals an asymptotic 3dB gap between noncoherent detection of DPSK and coherent detection in generalized diversity Rayleigh fading channels channels. (This gap is also found–by other analytical means–in [3].) Prior to that, this 3dB gap was known only for the special case of uncorrelated signals in independent and identical fading paths [11].

Since in the multiuser, slowly fading case the asymptotic BER does not depend on the interfering users' energies, the near-far resistance coincides with the asymptotic efficiency. The latter turns out to be in general smaller than unity, and hence the gap between noncoherent DPSK detection and coherent detection increases for multiple users, as was observed in [1]. For fast fading the error floor (which is reached only at high levels of the SNR) is bounded from below and above, where the bounds are seen numerically to be tight for relevant fade rates. The floor depends on the fade rate only.

In summary, the analysis presented in this paper allows us to succinctly quantify the performance of the MEP multiuser detector in that the non-trivial bounds on the BER can be replaced by more accessible asymptotic expressions.

REFERENCES

[1] M. K. Varanasi and M. Brehler, "A systematic approach to noncoherent detection for DPSK modulation in multiuser correlated diversity Rayleigh fading channels," in *Proc. Conf. Inform. Sciences and Systems*. Princeton University, Mar. 1998, pp. 236–241.

[2] M. K. Varanasi, "A systematic approach to noncoherent detection for DPSK modulation in single-user correlated diversity rayleigh fading channels with applications to post-combining decorrelative multiuser detection," in *Proc. Conf. Inform. Sciences and Systems*. Johns Hopkins University, Mar. 1997, pp. 480–485.

[3] M. K. Varanasi, "A systematic approach to the design and analysis of optimum DPSK receivers for generalized diversity communications over Rayleigh fading channels," *IEEE Trans. Commun.*, vol. 47, no. 9, pp. 1365–1375, Sept. 1999.

[4] M. Brehler and M. K. Varanasi, "A systematic approach to noncoherent detection for DPSK modulation in multiuser correlated diversity Rayleigh fading channels," Tech. Rep., University of Colorado, May 1998, also a Dipl.–Ing. thesis submitted to the Technische Universität München.

[5] M. K. Varanasi, "Parallel group detection for synchronous CDMA communication over frequency-selective Rayleigh fading channels," *IEEE Trans. Inform. Theory*, vol. 43, no. 1, pp. 116–128, Jan. 1996.

[6] M. Brehler and M. K. Varanasi, "Asymptotic error probability analysis of quadratic receivers in Rayleigh fading channels with applications to a unified analysis of coherent and noncoherent space-time receivers," submitted to *IEEE Trans. Inform. Theory*, Aug. 2000.

[7] M. Schwartz, W. R. Bennett, and S. Stein, *Communication Systems and Techniques*, An IEEE Press Classic Reissue, New York, 1996, Originally A McGraw-Hill Publication, 1966.

[8] W. C. Jakes, *Microwave Mobile Communications*, An IEEE Press Classic Reissue, New York, 1993, Originally An American Telephone and Telegraph Company Publication, 1974.

[9] R. A. Horn and C. R. Johnson, *Matrix Analysis*, Cambridge University Press, 1993.

[10] C. W. Helstrom, *Elements of Signal Detection & Estimation*, Prentice-Hall, Englewood Cliffs, NJ, 1995.

[11] J. G. Proakis, *Digital Communications*, McGraw-Hill, New York, 3rd edition, 1995.

Some of the references are available in portable document and postscript format from `http://ece-www.colorado.edu/˜varanasi`

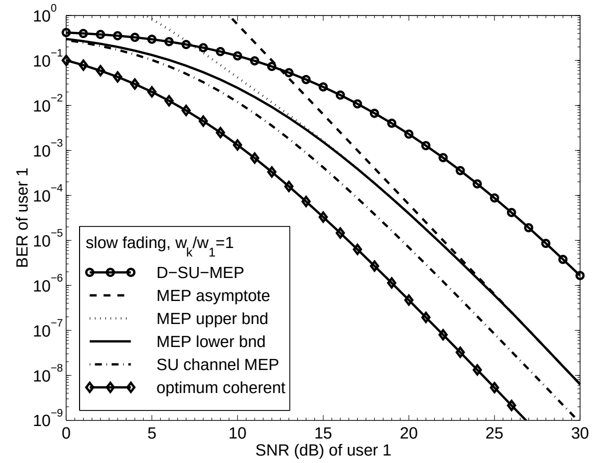

Fig. 1. BER comparison of the optimum multiuser DPSK, optimum multiuser coherent, and decorrelating DPSK detector.

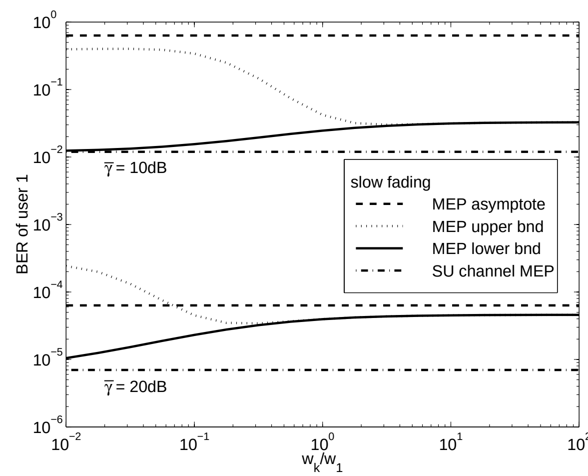

Fig. 2. The upper and lower bound on the BER of the first user as a function of the relative powers of the other users

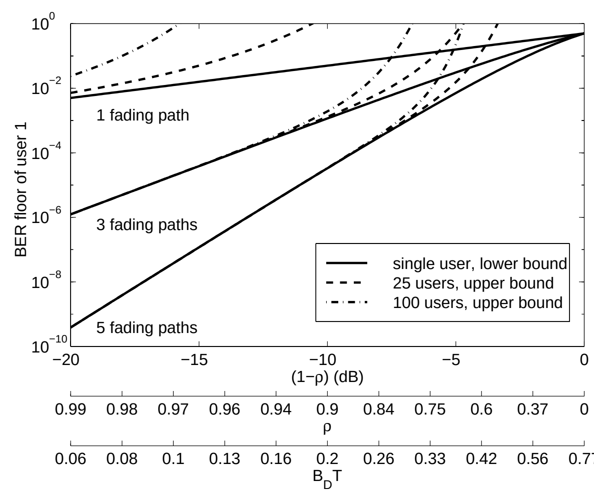

Fig. 3. BER floor of the optimum multiuser DPSK detector for SNR $\to \infty$ as a function of the fade rate